Infrared Imaging in Diagnosis of Dysplastic Nevi and Malignant Melanoma

Kızılötesi Işık ile Atipik Nevus ve Malign Melanom Tespiti

Burhan ENGİN,[a]
Ayşegül Sevim KEÇİCİ,[a]
Serdar YILMAZ,[b]
Zekayi KUTLUBAY,[a]
Server SERDAROĞLU,[a]
Yalçın TÜZÜN[a]

[a]Department of Dermatology and
Venereology,
İstanbul University
Cerrahpaşa Faculty of Medicine,
[b]Department of Electrical and
Electronics Engineering,
Fatih University Faculty of Engineering,
İstanbul

Yazışma Adresi/*Correspondence:*
Burhan ENGİN
İstanbul University
Cerrahpaşa Faculty of Medicine,
Department of Dermatology and
Venereology, İstanbul,
TÜRKİYE/TURKEY
burhanengin2000@yahoo.com

ABSTRACT Objective: The aim of this study is to handle the subjectivity of clinical observations in the diagnosis of dysplastic nevi and malignant melanoma, by using an alternative spectrophotometric method to simple dermatoscopic examination. **Material and Methods:** Images taken by CCD (Charge-coupled Device) camera with a 1280x1024 pixel resolution which is capable of taking snapshot images between 400-1000 nm wavelengths were converted to 2048x2560 size data and were subjected to digital image processing. For each lesion, three different images were captured at selected infrared wavelengths of 770 nm, 810 nm, 850 nm and one image with visible light. Risk score analysis of the digital image processing was carried out on two main parameters. One is surface area risk score (SAR) and the other is pixel intensity risk score (PIR). The same lesions are also evaluated dermatoscopically and ABCD scores of each lesion were calculated. **Results:** Thirty nine patients with 47 pigmented lesions were included in the study. When all the statistical data were put together, positive correlation with ABCD scores is stronger for the images at 770 nm than the ones with 810 nm. Also when we consider all parameters which have been studied separately, the most meaningful correlation with ABCD scores was shown by "total surface area risk score". **Conclusion:** Wavelengths of 770 nm and 850 nm seem to be optimal in terms of correlating with ABCD scores of the lesions. Also we need to determine the optimum wavelength range for the accurate diagnosis of melanocytic lesions.

Key Words: Melanoma; nevus

ÖZET Amaç: Bu çalışmanın amacı displastik nevus ve malign melanom tanısında ilk basamak olan rutin dermatoskopinin yerine alternatif spektrofotometrik yöntemler kullanılarak klinik gözlemlerdeki subjektifliği (öznelliği) azaltmaktır. **Gereç ve Yöntemler:** 400-1000 nm arasında görüntü kaydedebilen ve 1280x1024 piksel çözünürlükte çekim yapan CCD (Charge-coupled Device) kamera ile elde edilen görüntüler, 2048x2560 büyüklükte dataya çevrilmiş ve dijital görüntüleme işlemlerine tabi tutulmuştur. Her lezyon için 770 nm, 810 nm ve 850 nm dalga boylarında ve görünür ışıkta olmak üzere dört farklı resim çekilmiştir. Dijital görüntüleme işlemleri sırasında risk skor analizleri iki parametreye göre yapılmıştır; yüzey alanı risk skoru (SAR) ve piksel yoğunluk risk skoru (PIR). Her lezyon için dermatoskopik inceleme de yapılmış ve ABCD skorları hesaplanmıştır. **Bulgular:** Çalışmaya toplamda 47 pigmente lezyona sahip 39 hasta dahil edilmiştir. İstatistik analizler sonucunda, kızılötesi görüntülerle ABCD skorları arasındaki ilişki 770 nm'de 810 nm'ye göre daha kuvvetli olarak saptanmıştır. Yine çalışılan tüm parametrelere bakıldığında, ABCD skoruyla "total yüzey alan risk skoru" arasındaki ilişki en yüksek bulunmuştur. **Sonuç:** Lezyonların ABCD skorları 770 ve 810 nm dalga boylarındaki görüntüleri diğer dalga boylarına göre daha anlamlı bir ilişkiye sahiptir. Melanositik lezyonların tanısında en uygun dalga boyunun saptanması için ileri çalışmalara ihtiyaç vardır.

Anahtar Kelimeler: Melanom; nevüs

The increased incidence of malignant melanoma all over the world makes it very important for both primary care physicians and dermatology specialists to recognize this condition for early interventions.[1] Clinical diagnosis of both melanoma and its precursor dysplastic nevi depend mainly on examination of color and shape of the suspected lesions. Therefore it is very probable that inter-physician variations will not only affect the excision decisions, but also consecutively the prognostic pathways.

In recent years, new technological methods have been proposed to overcome the problem of accurate and rapid diagnostic approaches. Many of these techniques are based on computer image analysis, in order to obtain quantitative measurements in an objective and reproducible fashion.[2]

The aim of this study was to establish a standardized diagnostic methodology for both the dysplastic nevi and melanoma. For this purpose, we used infrared imaging techniques based on the analysis of a sequence of multispectral images of a lesion, with the help of a computer-based algorithm. The reason that makes infrared imaging convenient is the fact that it constitutes a functional and non-invasive imaging method.[3] Those data regarding the infrared images were collected and a comparison of each lesion with the classical ABCD scoring system was made. In selective cases, if there is any suspicion of dysplastic nevi or melanoma, histopathological examinations (Table 1) are also conducted, with complete excision of the lesion.

MATERIAL AND METHODS

1. STUDY POPULATION

Forty-one patients were included in our study initially, but two patients were lost to follow-up. Thus thirty-nine patients (20 males, 19 females), with 47 pigmented lesions were recruited from the dermatology department of Cerrahpasa Medical Faculty, Istanbul University between the period of January 2014 and June 2014. The average age of the patients was 47 (range between 19 and 67). Localizations of the lesions are shown in details, in Table 1. The maximum diameter of the lesions ranged from 0.3 to 2.2 cm. The patients were questioned for a previous cumulative ultraviolet radiation exposure, continuous or intermittent. Also family histories of skin cancer, patients' comorbidities, with drug use and systemic diseases, history of previous immunosuppressive treatments were taken into consideration (Table 1).

The local ethical committee has approved the clinical study.

2. ABCD SCORE CALCULATION

ABCD score of each lesion was calculated by the criteria including asymmetry, border, color and dermoscopic structures. For asymmetry, two 90° axes that were positioned to produce the lowest possible asymmetry score bisected the melanocytic lesion. If both axes show dermoscopically asymmetric contours with regard to shape, colors and/or dermoscopic structures, the asymmetry score was 2. For the border evaluation, the lesion was divided into eight. Within each one-eigth segment, a sharp, abrupt cut-off of pigment pattern at the periphery received a score of 1. Therefore the maximum border score was 8. Six different colors were determined for the maximum color of 6.

Evaluation of dermoscopic structures focuses on five structural features: network, structureless (or homogeneous) areas, branched streaks, dots and globules. Structureless (or homogenous) areas must be larger than 10% of the lesion to be considered present. Branched streaks and dots are counted only when more than two are clearly visible. The presence of a single globule is sufficient for the lesion to be considered positive for globules.[4-8]

3. IMAGING SYSTEM

The image acquisition system consists of a CCD (Charge-coupled Device) camera with 1280x1024 pixel resolution. The CCD camera has a zooming feature of 10-70 times magnification manually and 200 times magnification digitally. The camera is capable of taking snapshot images between 400 nm and 1000 nm wavelengths; in case of visible light between 400-700 nm and near-infrared pictures between 700-1000 nm. The camera can take snap-

Patients	Location	ABCD scores	Skin cancer Family history	Comorbidity	Immunosupressive treatment	Histopathology
TABLE 1: Location of lesions, ABCD scores, histopathology and demographical features.						
1	Left arm	2.5	-	-	-	
2	Back	2.9	-	-	-	
3	Toe	7.2	-	DM	-	M
4	Ankle	4.1	-	-	-	
5	Back	4.8	-	-	-	MN
6	Toe	3	-	-	-	
7	Left thigh	1.6	-	HT	-	
7	Back	3	-	HT	-	
8	Face	3.5	-	-	-	
9	Back	5.9	+ (BCC)	-	-	
10	Nose	2.6	-	-	-	
11	Right arm	3	-	-	-	
12	Left leg	3	-	-	-	
13	Back	2.9	-	-	-	
14	Right leg	2.2	-	-	-	
15	Abdomen	2.2	-	-	-	CN
16	Back	4.2	-	HT	-	
16	Face	2.5	-	HT	-	
17	Right thigh	4	-	-	-	
18	Right leg	5.1	-	-	-	
19	Abdomen	1.6	-	-	-	
19	Abdomen	2.9	-	-	-	
20	Left leg	2.7	-	-	-	MN
21	Right thigh	3.1	+ (BCC)	DM	-	
22	Back	2.6	-	-	-	
23	Abdomen	4.7	-	-	-	
24	Right thigh	3.3	-	-	-	
25	Chest	3.3	-	-	-	
25	Abdomen	4.9	-	-	-	
26	Left thigh	5.2	-	Psoriasis	Cyclosporine	DN
27	Right leg	3.8	-	-	-	DeN
28	Back	5.4	-	-	-	
29	Left leg	4.9	+ (M)	-	-	
30	Face	4.6	-	-	-	DN
31	Back	6	-	Depresion	-	
32	Right leg	6.1	-	-	-	LM
32	Abdomen	6	-	-	-	MN
33	Chest	6	-	-	-	
33	Right leg	4.9	-	-	-	
34	Shoulder	5.4	+ (BCC)	-	-	
35	Back	5.8	-	HT, HL	-	MN
35	Right thigh	5.3	-	HT, HL	-	
36	Shoulder	6.5	-	-	-	DN
37	Left leg	3.6	-	-	-	
38	Shoulder	4	+ (SCC)	-	-	
39	Face	5.3	+ (SCC)	-	-	

M: Melanoma; BCC: Basal cell carcinoma; SCC: Squamous cell carcinoma; MN: Melanocytic nevus; DN: Dysplastic nevus; LM: Lentigo maligna; CN: Compound nevus;
DeN: Dermal nevus; DM: Diabetes Mellitus; HT: Hypertension; HL: Hyperlipidemia.

shot images in four different wavelengths. Four various wavelength snapshots were taken for each lesion. First, 400-700 nm visible light wavelength images were taken as a reference. Then 770 nm, 810 nm and 850 nm infrared wavelength snapshots were taken respectively.

In Figure 1, visible light and infrared images of two selected lesions can be observed (Figure 1a, b).

4. DIGITAL IMAGE PROCESSING AND ANALYSIS

Images taken at wavelengths between 400-1000 nm were converted to 2048x2560 size data and are subjected to digital image processing. Risk score analysis of the digital image processing was carried out on two main parameters. One is surface area risk score (SAR) and the other is pixel intensity risk score (PIR) for each 770 nm, 810 nm and 850 nm infrared wavelength images.

All details of SAR and PIR scores and their calculation methods were evaluated on following sections.

Surface Area Risk (SAR) Scores for Infrared Wavelength Images

Pixel area (PA) of each infrared image was calculated by image processing techniques; edge detection with effective threshold and counting pixel of the lesions. These scores were recorded as PA_{770nm}, PA_{810nm} and PA_{850nm}. Subsequently, we normalized SAR score by visible light image area (VIA)

score. Finally each SAR score was as SAR_{770nm}, SAR_{810nm} and SAR_{850nm}.

SAR score of each infrared images were calculated by x subscript for 770, 810 and 850 nm wavelengths.

$$SAR_x \quad \frac{PA_x}{VIA}$$

Pixel Intensity Risk (PIR) Score for Infrared Wavelength Images

Pixel intensity risk (PIR) score of each infrared image was calculated by image processing techniques; edge detection with effective threshold and mean pixel intensity of lesion. Total pixel intensity (TPI) was the value of pixel density corresponding to the lesion area. Finally each score was recorded as PIR_{770nm}, PIR_{810nm} and PIR_{850nm}.

$$PIR_x \quad \frac{TPI_x}{PA_x}$$

5. STATISTICAL ANALYSIS

For the statistical study analysis between ABCD scores versus infrared SAR and PIR scores, following correlation tests were used; Spearman Correlation (SC), Linear Correlation (LC), Root Mean Square Root Error (RMSE). Kendall's rank correlation was also calculated but the values were similar
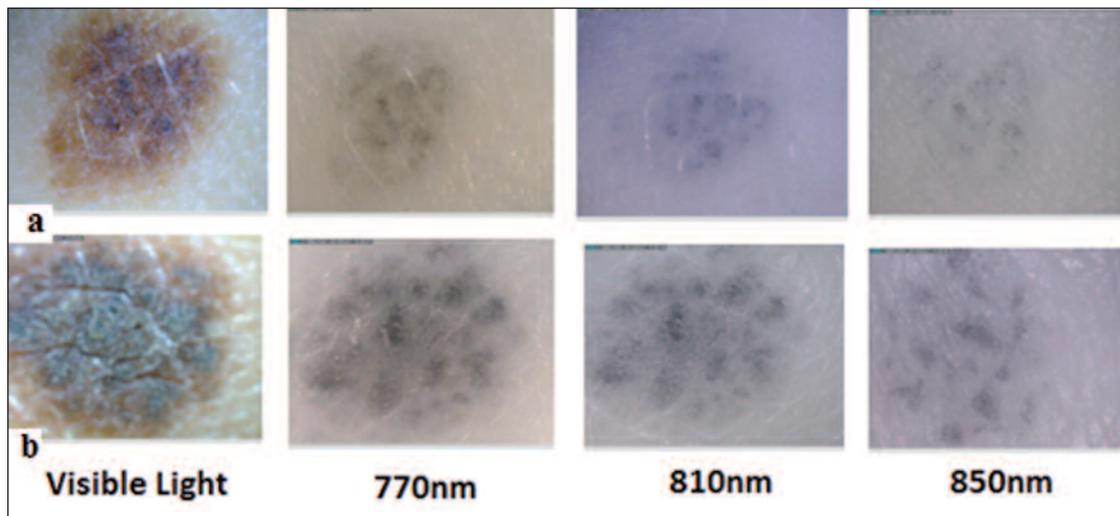
FIGURE 1A, B: Visible light and infrared images of two selected lesions at 770, 810 and 850 nm.

to Spearman correlation. Use of more than one statistical test aims at establishing the possible relationship between our ABCD score data set and image values and eventually classification of more advanced infrared imaging techniques.

Spearman Correlation (SC) was used for the evaluation of the relationship between two different sets of data for the proof of presence and strength of the relationship. Linear correlation (LC) was used for the strength and direction of the linear relationship between statistically different sets of data. For measuring the differences between values predicted by a model or an estimator and the values actually observed, the root-mean-square error (RMSE) was used.

RESULTS

Thirty-nine patients (20 males, 19 females), with 47 pigmented lesions were included in our study, during a period of six months. Previous ultraviolet exposure, systemic diseases or history of previous immunosuppressive treatment were not correlated with the lesions ABCD scores or infrared imaging properties. Two patients had a family history of basal cell carcinoma, one squamous cell carcinoma and one patient had a family history of melanoma. Patients had concomitant diseases such as depression, hypertension, hyperlipidemia, diabetes and psoriasis. None of the patients were under immunosuppressive treatment at the time of the study, but one had previously used cyclosporine for psoriasis.

RELATIONSHIP BETWEEN TOTAL SAR SCORE AND ABCD SCORE

Individual SAR scores of 770nm and 850nm are more strongly correlated with ABCD scores than the ones with 810nm. When we take all the data gathered from the statistical analysis into account, for the SC, LC, RMSE, the most powerful relation was obtained with "Total SAR score", with 0.6913, 0.7053 and 0.5315 values respectively (Table 2). In case of LC analysis, total SAR scores and 850 nm images were more relevant. For the RMSE, again ABCD scores and total SAR score relationship had the most meaningful correlation, when compared to individual wavelength results.

The comparison of ABCD scores and Total SAR Scores is shown on scatter plots (Figure 2a, b, c and d). Figure 2 shows the scatter plot graphics of the relationship between SAR score and ABCD scores of the lesions. Total SAR score and the ABCD scores show a clear linear relation. However the relation between individual scores of 770nm, 810nm and 850nm and ABCD scores is not linear.

RELATIONSHIP BETWEEN PIR SCORES AND ABCD SCORE

PIR scores are negatively correlated with ABCD scores (Table 3). According to SC calculations, Total PIR score has the highest value but it still seems weakly correlated.

Figure 3 depicts lack of correlation between PIR and ABCD scores (Figures 3a, b, c and d). When we take the previous analysis of SAR score versus ABCD scores into account, there is a less strong correlation in case of PIR and ABCD scores.

DISCUSSION

Infrared imaging system is an accurate screening tool, which yields noninvasive and simple visualization of the skin. This system has long been used for the detection of melanocytes on the skin.[9-12] Images using various spectral bands from 420 to 1040 nm to enhance the ABCD criteria has been shown to improve the accuracy of detecting melanoma.[13-15] In our series for this purpose 47

TABLE 2: ABCD Scores vs Surface Area Risk Score (SAR).			
	SAR 770nm	**SAR 810nm**	**SAR 850nm**	**Total SAR**
SC (r_s)	0.6229	0.5456	0.5937	0.6913
LC (P_{xy})	0.5763	0.4244	0.6115	0.7053
RMSE (e)	0.6365	0.6526	0.6759	0.5315

SC: Spearman correlation; LC: Linear correlation; RMSE: Root mean square root error.

TABLE 3: ABCD Scores vs Pixel Intensity Risk Score.			
	PIR 770nm	**PIR 810nm**	**PIR 850nm**	**Total PIR**
SC (r_s)	-0.3350	-0.4351	-0.4060	-0.4585
LC (P_{xy})	-0.3620	-0.3660	-0.3801	-0.3978
RMSE (e)	0.6515	0.6521	0.6493	0.5031

SC: Spearman correlation; LC: Linear correlation; RMSE: Root mean square root error.
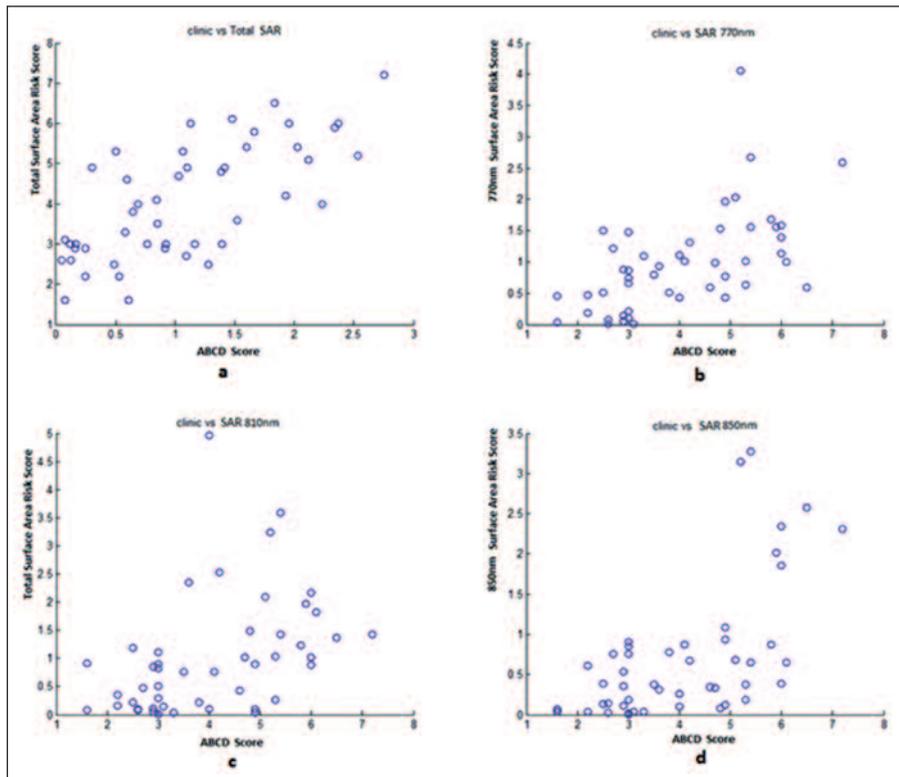
FIGURE 2: a, b, c and **d.** SAR Score Scatter Plots vs. ABCD Score.

pigmented lesions of thirty-nine patients were evaluated.

SAR scores of 770nm and 850nm gave more discriminating results, in case of ABCD score correlation. When we further investigate the association, total SAR scores which have been obtained from the infrared images, statistically had the most powerful relation with ABCD scores of each corresponding lesion. Each wavelength grants data from different layers of the skin, thus when more than one wavelength is involved, as in the case of total SAR score, the data becomes more powerful and correlates better with the ABCD scores.

On the other hand, PIR scores are negatively correlated with ABCD scores and there is a weaker association when compared to total SAR scores. Although wavelengths of 770 nm and 810 nm seem to be optimal for our study, the optimum wavelength range need to be determined for the accurate diagnosis of melanocytic lesions.

Infrared measurements are linked to the optical properties of the skin and they are the result of

light absorption, scattering, and emission. At this point, both the color and the thickness of the lesions, as well as total melanin content of the epidermis and papillary dermis, collagen and hemoglobin content affects the infrared image signals that will be eventually produced.[16,17] In our study, we convert the infrared images to mathematical values, based on the surface area of the lesions and pixel intensity. In this way, different values of different wavelengths could be compared. Use of two dimensional and gray scale images made the calculations more accurate. There was some difficulty for some lesions due to the inconsistency of infrared image pixel density and their ABCD scores, which disrupted the linearity of the data.

Total excision was made for 14 of these lesions, with results of five dysplastic nevi, one lentigo maligna and two melanomas. ABCD scores of these lesions were relatively high, which evoke the clinical suspicion for excision decision. Infrared imaging scores were also compatible with the ABCD scores. Mean ABCD score of these 14 lesion was as high as 5.24. The exci-
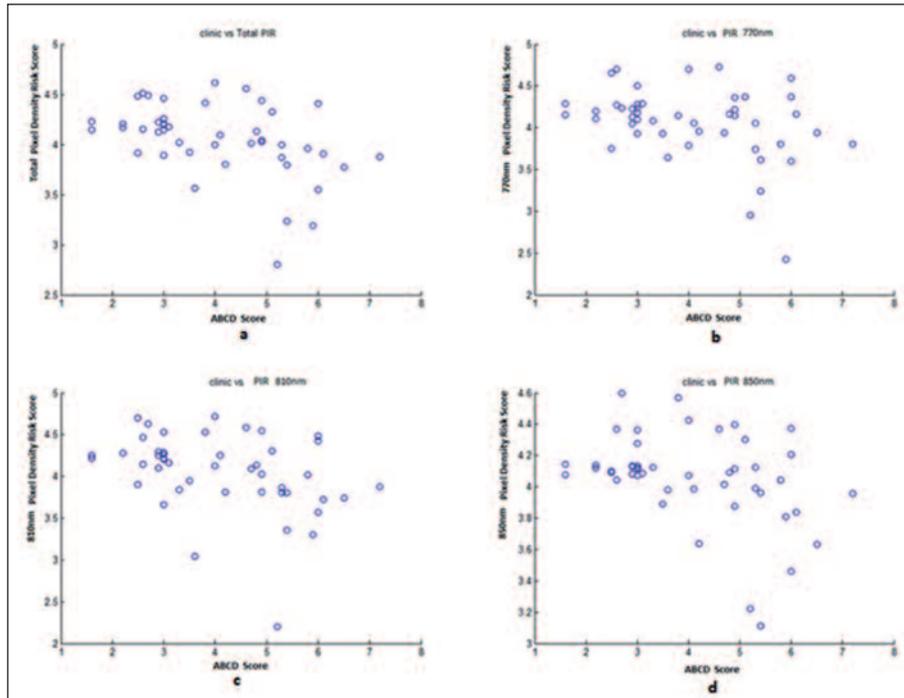
FIGURE 3: a, b, c and **d.** PIR Score Scatter Plots vs. ABCD Score.

sion decision was first made on these scores but during the infrared imaging process, infrared scores also supported the initial ABCD scores.

The most important limitation of infrared imaging technology is detection of optimum wavelength value. Each wavelength reaches a different layer of the epidermis and dermis, thus grants the image data of that layer.[18] Therefore more than one wavelength calculation is crucial for detailed image of the whole skin thickness.

In conclusion, the evolving technique of in vivo use of infrared imaging technology widens the diagnostic field of dermatology. The result of this study supports many others, on the area of multispectral imaging approaches for all kinds of melanocytic lesions, from simple nevi to malignant melanomas. During the clinical approach to melanocytic lesions, infrared imaging can be a supportive diagnostic tool to routine dermatoscopical examination.

▌REFERENCES

1. Jemal A, Devesa SS, Fears TR, Hartge P. Cancer surveillance series: changing patterns of cutaneous malignant melanoma mortality rates among whites in the United States. J Natl Cancer Inst 2000;92(10):811-8.

2. van Engen-van Grunsven AC, Kusters-Vandevelde H, Groenen PJ, Blokx WA. Update on molecular pathology of cutaneous melanocytic lesions: what is new in diagnosis and molecular testing for treatment? Front Med (Lausanne) 2014;1(1):39.

3. Ugarte MF, Chávarri L, Briz S, Padrón VM, García-Cuesta E. Active multispectral imaging system for photodiagnosis and personalized phototherapies. Rev Sci Instrum 2014;85(10):105108.

4. Pellacani G, Grana C, Seidenari S. Algorithmic reproduction of asymmetry and border cut-off parameters according to the ABCD rule for dermoscopy. J Eur Acad Dermatol Venereol 2006;20(10):121-49.

5. Roesch A, Burgdorf W, Stolz W, Landthaler M, Vogt T. Dermatoscopy of "dysplastic nevi": a beacon in diagnostic darkness. Eur J Dermatol 2006;16(5):479-93.

6. Carli P, de Giorgi V, Palli D, Giannotti V, Giannotti B. Preoperative assessment of melanoma thickness by ABCD score of der-matoscopy. J Am Acad Dermatol 2000;43(3):459-66.

7. Goodson AG, Grossman D. Strategies for early melanoma detection: approaches to the patient with nevi. J Am Acad Dermatol 2009;60(5):719-38.

8. Carli P, De Giorgi V, Massi D, Giannotti B. The role of pattern analysis and the ABCD rule of dermoscopy in the detection of histological atypia in melanocytic naevi. Br J Dermatol 2000;143(2):290-7.

9. Santa Cruz GA, Bertotti J, Marín J, González SJ, Gossio S, Alvarez D, et al. Dynamic infrared imaging of cutaneous melanoma and

normal skin in patients treated with BNCT. Appl Radiat Isot 2009;67(7-8 Suppl):S54-8.

10. A'Amar OM, Ley RD, Bigio IJ. Comparison between ultraviolet-visible and near-infrared elastic scattering spectroscopy of chemically induced melanomas in an animal model. J Biomed Opt 2004;9(6):1320-6.

11. Mcintosh LM, Summers R, Jackson M, Mantsch HH, Mansfield JR, Howlett M, et al. Towards non-invasive screening of skin lesions by near-infrared spectroscopy. J Invest Dermatol 2001;116(1):175-81.

12. Tomatis S, Carrara M, Bono A, Bartoli C, Lualdi M, Tragni G, et al. Automated melanoma detection with a novel multispectral imaging

system: results of a prospective study. Phys Med Biol 2005;50(8):1675-87.

13. Bono A, Tomatis S, Bartoli C, Cascinelli N, Clemente C, Cupeta C, et al. The invisible colours of melanoma. A telespectrophotometric diagnostic approach on pigmented skin lesions. Eur J Cancer 1996;32(4):727-9.

14. Tomatis S, Bartoli C, Bono A, Cascinelli N, Clemente C, Marchesini R. Spectrophotometric imaging of cutaneous pigmented lesions: discriminant analysis,optical properties and histological characteristics. J Photochem Photobiol 1998;42(1):32-9.

15. Farina B, Bartoli C, Bono A, Colombo A, Lualdi M, Tragni G, et al. Multispectral imaging ap-

proach in the diagnosis of cutaneous melanoma: potentiality and limits. Phys Med Biol 2000;45(5):1243-54.

16. Bigio IJ, Mourant JR. Ultraviolet and visible spectroscopies for tissue diagnostics: fluorescence spectroscopy and elastic-scattering spectroscopy. Phys Med Biol 1997;42(5):803-14.

17. Wolbarsht ML, Walsh AW, George G. Melanin, a unique biological absorber. Appl Opt 1981;20(13):2184-6.

18. Murray CS, Stockton DL, Doherty VR. Thick melanoma: the challenge persists. Br J Dermatol 2005;152(1):104-9.